Evolution to Modernized GNSS Ionospheric Scintillation and TEC Monitoring

Surendran Shanmugam, Jason Jones, and Allan MacAulay
NovAtel Inc.,
Calgary, Alberta, Canada

A.J. Van Dierendonck
AJ Systems/GPS Silicon Valley
Los Altos, CA, United States

Abstract— The ionosphere, if not modeled sufficiently well, is the largest contributor of error in single frequency GNSS receivers. Modeling ionospheric effects is a major concern for a number of GNSS applications. Ionospheric disturbances induce rapid fluctuations in the phase and the amplitude of received GNSS signals. These rapid fluctuations or scintillation potentially introduce cycle slips, degrade range measurements, and if severe enough lead to loss of lock in phase and code. GNSS signals, although vulnerable, themselves provide an excellent way to measure the ionospheric effect continuously worldwide. Until now, ionospheric monitoring was performed using receivers such as the GSV4004B receiver, which was largely based on GPS only dual frequency receivers. Semi-codeless tracking of the GPS L2 signal greatly limited the accuracy, robustness and utility of the ionospheric TEC measurements and was useless for scintillation measurements on L2. The GPS modernization program, the restored GLONASS, and the upcoming GNSS constellations (Galileo and Compass) bring forth huge benefits for ionospheric monitoring. This paper introduces the NovAtel's next generation GNSS ionospheric scintillation and TEC monitor, the GPStation-6. By incorporating the proven GSV4004B receiver design with the ability to track multi-constellation, multi-frequency, GNSS measurements, the new receiver engine provides robust and less noisy ionospheric measurements.

Keywords-ionosphere; GNSS; amplitude scintillation; phase scintillation; total electron content (TEC); space weather; monitoring.

I. INTRODUCTION

Global navigation satellite system (GNSS) is a system of satellite systems providing all-weather continuous position, navigation and time (PNT) information with greater accuracy worldwide. GNSS has now become quintessential to a wide range of industrial applications from construction and surveying, aviation, precision agriculture to earth sciences and even space weather research [1]. GNSS like any other satellite systems is vulnerable to space weather [2]. This is of particular concern for safety-of-life applications that rely on the integrity, accuracy, and availability of GNSS [3].

Unmodeled ionospheric delay is usually the largest and variable cause of error in single frequency GNSS receivers [4]. Unlike the troposphere, the ionosphere is a dispersive medium that is predominant with electrically charged atoms and molecules (ions) and free electrons formed primarily due to ionization by solar radiation [5]. The ionosphere exhibits both diurnal and seasonal effects originating from solar activity [6-8]. The Sun enters a period of increased activity approximately every eleven years called the solar maximum, which influences the amount of irradiance received from Sun on earth. The impending solar maximum is expected in 2013 [8]. Solar maximum is associated with increased solar flares (of powerful X types) and coronal mass ejection that causes intense disturbances of earth's magnetosphere temporarily [7].

Geographical regions, including the polar (at auroral latitudes) and Equatorial regions (± 20 degrees of geomagnetic Equator), predominantly witness increased ionospheric activity. The ionospheric activity in polar region is primarily associated with geomagnetic storms, coronal mass ejections and coronal holes [9]. On the other hand, the equatorial ionospheric activity mostly occurs during post sunset period due to the equatorial electrojet current system and its instabilities, the equatorial ionization anomaly (EIA), and the instabilities or irregularities in equatorial plasma of the night ionosphere [10]. The ionospheric irregularities caused by equatorial anomaly take place more frequently and severely during the period of solar maximum. During these solar events, the ionosphere disturbances disrupt radio propagation in satellite based communication and navigation systems [11].

The presence of free electrons in the ionosphere imparts delay on the received GNSS signal. The GNSS code and carrier are affected differently as the signal interacts with the free electrons, along its transmission path through the ionosphere. The presence of the free electrons making up the ionosphere alters the refractive index of the atmosphere. The phase refractive index of ionosphere is less than unity and thus "advances" the phase of the carrier component. On the other hand, the code component is "delayed" (group delay) as the refractive index of ionosphere is greater than unity. Besides, the magnitude of this carrier advance and code delay is proportional to the refractive index of ionosphere in the GNSS signal path. The refractive index in turn is affected by the total electron content (TEC) of the ionosphere in the GNSS signal path. TEC is highly variable both spatially and temporally.

Ionospheric irregularities where the electron density can differ significantly from the ambient plasma cause diffraction of radio signals [11]. Accordingly, the received GNSS signals experience rapid temporal fluctuations in both amplitude and

phase known as the "ionospheric scintillation" [4]. Amplitude scintillation can degrade both pseudorange and carrier phase measurements and thus affecting the GNSS signal quality. Deep signal fades over sufficient duration can cause loss of lock in both code and carrier [12]. Secondly, strong phase scintillation can readily stress phase-lock loops (PLL) in GNSS receivers resulting in a loss of phase lock and frequent cycle slips, thereby impeding carrier phase measurements [13].

Single frequency GNSS receivers use broadcast correction data based on ionospheric models, such as the Klobuchar model, used by Global Positioning System (GPS) and NeQuick model that will be adopted in Galileo system [14]. Unfortunately, the ionospheric corrections from these models are limited during high ionospheric activity. Improved ionospheric corrections can be attained using the broadcast data from satellite based augmentation systems (SBAS) such as the US WAAS, the European EGNOS, the Japanese MSAS, and the future Indian GAGAN [15]. These SBAS systems provide ionospheric delay corrections along with integrity/accuracy data on those corrections known as the grid ionospheric vertical error (GIVE). GIVE characterizes the residual error in the ionospheric corrections for the estimated ionospheric delays over several strategically located ionospheric grid points (IGP) [3]. Nonetheless, during ionospheric events, the augmentation systems are unable to provide accurate vertical guidance, leaving safety critical users with horizontal guidance alone. Besides, augmentation systems are themselves vulnerable in equatorial regions [16].

GNSS systems broadcast signals on more than one frequency so that a correction of the delay through the ionosphere can be determined. For instance, dual frequency GPS receivers track L1/L2 signals to form ionosphere-free pseudorange and carrier phase observables. This ionosphere free combination is effective in mitigating the error due to the first order ionospheric effect. While the first order ionospheric term accounts for tens of metre compared to higher order errors, the higher order ionospheric effects are becoming more relevant with growing precision GNSS applications. Precise carrier phase positioning is particularly vulnerable to any ionospheric effects [17]. The ability to resolve ambiguities in real time kinematic (RTK) positioning can be influenced by the ionospheric effects even for short baselines. Finally, sub-metre level precise point positioning (PPP) using single frequency is largely influenced by ionospheric effects.

Until recently, only the encrypted GPS L2 P(Y) signal was available for measuring the delay through the ionosphere. Accordingly, the GPS receivers utilized semi-codeless techniques to track the encrypted L2 P(Y) signal. The signal-to-noise ratio (SNR) loss from semi-codeless tracking can be anywhere between 15 and 35 dB and further depends on the L1 tracking quality [18]. Modernized GNSS will alleviate this problem using new civilian GPS signals.

GNSS signals despite being vulnerable to ionosphere effects provide an excellent mean for ionospheric monitoring on a global basis in a continuous fashion [5]. Secondly, with multiple satellites, the ionospheric effect can be measured through many pierce points simultaneously. Single or dual frequency GNSS receivers with configurable carrier tracking loop bandwidth have been traditionally used as Ionospheric scintillation monitors (ISM) [20]. The use of wide carrier loop noise bandwidths can help maintain phase tracking during periods of ionospheric phase scintillation by tracking rapidly changing phase. On the other hand, narrow carrier loop noise bandwidth is desirable to tolerate amplitude scintillation with the ability to track at lower C/N_0 conditions, or to "fly-wheel" through the deep fades [20].

Ionospheric effects are typically characterized by measuring its impact on amplitude and phase of the received GNSS signal. The most widely considered measures are the scintillation indices (i.e. amplitude and phase), and the TEC [18]. The amplitude scintillation index, or the S_4 index, measures the standard deviation of the normalized signal intensity, typically over a 60 second period. Both amplitude and phase scintillation measurements should be detrended to extract the contribution from scintillation alone, while attempting to reject the effects of signal dynamics and multipath. TEC measurements can be obtained by differencing pseudorange and carrier phase observables between two frequencies broadcasted from the same satellite. TEC measurements based on carrier phase are accurate but ambiguous. Code based measurement provides an absolute yet noisy TEC values. Carrier aiding of code loop is typically used to reduce the noise in code based TEC measurements, along with carrier TEC smoothing of the code TEC measurements.

The GPS modernization, the restored Russian GLONASS, and the upcoming European Galileo and Chinese Compass GNSS brings forth immense benefits and challenges for ionospheric monitoring. The new civilian signals broadcasted at multiple frequencies enable better ionospheric measurements through multitude pierce points. However, the complex structure of the new signals and the sheer number of available signals at multiple frequencies necessitate robust and yet stable receiver technology.

Motivated by the above, NovAtel, Inc. has developed a new GNSS Ionospheric Scintillation and TEC Monitor (GISTM), the GPStation-6[TM]. This paper describes the benefits of the new GISTM receiver compared to traditional single/dual frequency single frequency GPS monitors for ionospheric scintillation monitoring. The paper has been organized as follows. Section II reviews the evolution of GPS based scintillation monitors. Section III outlines the salient features of the GPStation-6 based scintillation monitoring. Preliminary results from a recent measurement campaign are presented in Section IV. Concluding remarks are summarized in Section V.

II. GNSS Ionospheric Scintillation Monitor Evolution

In the mid 1990s, on Small Business Innovative Research (SBIR) contracts with the Air Force Research Laboratory (AFRL) [19], an Ionospheric Scintillation Monitor Receiver was developed by GPS Silicon Valley with support from NovAtel, Inc., via modifications to a standard NovAtel GPS receiver (L1 only), known as the GPStation that was normally used in differential GPS applications as a reference receiver. It was packaged in an enclosure along with a low phase noise

AT-Cut Oven-Controlled-Crystal-Oscillator (OCXO) (for stable differential corrections, and, here, for measuring phase scintillation). The receiver's firmware was modified to add ionospheric scintillation indices, the associated data processing algorithms and the data logs to the standard GPS receiver firmware. Subsequently, the GPS receiver was able to provide ionospheric measurements preferred by ionosphere research community that characterized ionosphere anomalies. Fifteen of these units were delivered to AFRL.

Unfortunately, the AT-Cut OCXO had a performance issue in that it exhibited "frequency popping," thought to be caused by a change in oven temperature, the influence of spurious resonance with step temperature characteristics, or change in oscillation circuit parameters, causing small shifts in oscillator frequency [21]. This phenomenon, when it occurred, caused the firmware-based phase detrending filters to "ring" in such a way that the phase scintillation parameters had no meaning. Fortunately, through a screening process, the fifteen units were successfully delivered.

Later, a second version of the scintillation monitor was developed that used standard 5 or 10 MHz OCXOs coupled with a frequency converter card (GSV 3001/3002), also developed by GPS Silicon Valley, which converted 5 or 10 MHz to the 20.473 MHz reference used in the receivers. In this configuration the popping never occurred, primarily because the OCXOs were of the SC-Cut variety, and operated at the lower frequencies closer to their natural frequency. Unfortunately, the GPStation physical format could no longer be used because of the additional frequency converter card. These new units (named the GSV4000 ISM) utilized the NovAtel 3951 PC Card receivers and were housed inside a personal computer using an ISA PC card slot. Industrial PCs were normally used. However, because of this more cumbersome configuration, the production and sales of the GSV4000 was somewhat limited. Only 19 units were built and sold.

These earlier scintillation monitors were limited to the GPS L1-C/A signal only. Around the year 2000, NovAtel GPS receiver technology modernized with the OEM4 GPS L1/L2 platform, and the original scintillation monitors evolved to the GSV4004 series (the GSV4004 and the GSV4004A and B) with the dual-frequency OEM4-G2 GPS receiver as its measurement engine. (The NovAtel OEM3 L1/L2 receivers existed before this, but they did not have the processor throughput for the scintillation index computations.) They all had dual-frequency tracking that provided the capability to measure TEC of the ionosphere. In addition, these platforms offered improved GPS receiver tracking including the ability to track SBAS GEO satellite signals, a very important feature allowing the measurement of ionospheric disturbances as they pass through signal pierce points in the Equatorial Region. Since 2004, nearly 350 of the popular GSV4004X series (GSV4004, GSV4004A and GSV4004B) units have been manufactured by NovAtel for GPS Silicon Valley (GSV) according to GSV specifications incorporating the custom GSV algorithms. GSV sold these GSV4004X GISTM receivers to scientific customers worldwide through 2011, when it was discontinued in lieu of GNSS signal modernization.

More recently, NovAtel Inc. launched the modernized GISTM receiver, the GPStation-6, for better ionospheric monitoring [22]. The multi-frequency multi-constellation GPStation-6 provide significant benefits while ensuring compatibility to the mature GPS L1/L2 only GSV4004B receiver described above for transition ease. Customizable software and utilities were based upon the GSV4004B software and thus readily supports existing workflows.

III. IONOSPHERIC SCINTILLATION MONITORING WITH GPSTATION-6

GPStation-6 is the next generation multi-frequency multi-constellation GISTM receiver based on the earlier generation GSV4004X receivers. The new GISTM receiver uses the NovAtel's advanced OEM628 GNSS measurement engine. The new measurement engine comprises of 120 independent channels and supports L1, L2 and L5 frequencies. GPStation-6 software is field upgradable to meet custom performance and needs. The receiver is capable of tracking all present and future GNSS constellations such as the GPS, GLONASS, Galileo, and Compass as well as the SBAS systems. Additional utilities facilitate automated receiver configuration, control, log decoding, post-processing algorithms and real-time data display. The GPStation-6 receiver is designed to ensure backward compatibility with GSV4004X receiver family.

GPStation-6, with a maximum sampling rate of 50 Hz readily supports high-rate ionospheric scintillation measurements. Physical raw signal intensity and phase noise spectral bandwidths of less than 25 Hz at the GNSS frequencies ensure that all the spectral components of amplitude and phase scintillation are measured. TABLE I summarizes the various features of the GPStation-6. The following subsections briefly outline the salient benefits that the new GISTM receiver brings forth in regards to ionospheric scintillation monitoring.

TABLE I. SUMMARY OF GPSTATION-6

Features	GISTM Receiver
Channel Configuration	120 independent channels
Signal Tracking	GPS (L1, semi-codeless L2P, L2C, L5) GLONASS (L1, L2-C/A, L2P) Galileo (E1, E5 A/B, E5 Altboc) SBAS (L1, L5) Compass (Upgradable)
Ionospheric Measurments	50 Hz phase and amplitude data (raw or detrended-raw)
Scintillation Indices (S_4, σ_ϕ)	GPS (L1 C/A, L2C, L5) GLONASS (L1, L2) Galileo (E1, E5) SBAS (L1, L5)
TEC (Code and Carrier)	GPS (L1/L2P, L1/L2C, L1/L5) GLONASS (L1/L2) Galileo (E1/E5A) SBAS (L1/L5) (1 Hz raw and 4/minute smoothed)
Communication Interface	USB/RS-232/RS-422 I/O (PPS, Event, Position Valid)

A. Multiple Frequency Measurments

Until recently, most GISTM receivers relied on semi-codeless L2 P(Y) tracking techniques to derive the dual frequency observables. On the other hand, the semi-codeless techniques incur squaring loss that is a function of L2 C/N_0. Even the best semi-codeless tracking incurs a squaring a loss of about 19 dB at a C/N_0 level of 30 dB-Hz [18]. Secondly, the semi-codeless techniques are heavily aided with the C/A code tracking to achieve very narrowband code and carrier tracking loops to minimize the inherent squaring loss. Therefore, given the typical 25-Hz spectral bandwidth of scintillation, good quality scintillation parameters are greatly limited due to the very use of the narrowband tracking loops. Thus, the semi-codeless measurements are only useful for TEC measurements.

The GPS modernization program commenced the beginning of new L2 and L5 civilian signals. The new GISTM receiver takes advantage of the clear-coded signals at L2 and L5 to derive true dual frequency observables. Hence, more robust and less noisy TEC measurements are now achievable in addition to the semi-codeless measurements. Finally, these modernized signals include a number of features that provide maximal benefits for ionospheric research community. For example, the new civilian L2C and L5 signal supports pilot component, better cross-correlation protection and advanced error correction that provides improved acquisition and tracking capabilities [25].

Among the modernized signals, the GPS L5 is of major importance. The received signal power of the L5 is at least 3.7 dB higher than L1 C/A, and is 5.1 dB higher in received power than the L2C signal. (L5 is another 0.9 dB higher on the future Block III GPS satellites, but the L2C signal power will also be 1.5 dB stronger on those satellites.) [26, 27]. The GPS L5 signal boasts a higher chipping rate (10.23 MHz) for robust tracking, better accuracy, improved multipath mitigation and much better interference resilience. Unlike the L2 signal, the L5 signal is part of the protected Aeronautical Radio Navigation Service (ARNS) band. However, the L2C signal brings immediate benefit as it is currently more available (9 GPS SV's) than the L5 signal (2 SV's). However, L5 is available on most current SBAS SVs, although not operational to the user, but is very available and important for amplitude scintillation monitoring in the Equatorial regions.

B. Multiple Constellation

Until recently, the U.S GPS was the only fully operational GNSS. Since October 2011, the Russian GLONASS restored its full coverage with the launch of 24th satellite of the system. The People's Republic of China is currently expanding its regional Beidou navigation system into the global Compass GNSS by 2020. The European Galileo GNSS system, after initial impediments, is now poised to have a full constellation by 2020. Finally, these GNSS systems will be broadcasting at multiple frequencies.

GPStation-6, with 120 independent channel configurations, is capable of tracking both the present and future constellations to generate ionospheric measurements. The ability to track more satellites greatly improves the number of pierce points through ionosphere that can be measured. The GPStation-6 supports upgradable software in the field to meet custom performance required for unique application demands.

C. SBAS Tracking

GPStation-6 receiver is capable of tracking SBAS satellites at both L1 and L5 frequencies. This provides huge benefits for users in the equatorial regions, where the ionosphere is not sufficiently modeled by the thin shell model and the planar approximations [23].

The phase and amplitude data collected from SBAS satellites have somewhat different characteristics than that collected from the GNSS satellites. First of all, the navigation data rate of the SBAS signal is 10-times higher than that of the GPS L1 signal. Adequate received signal power at Equatorial regions and advanced error correction readily compensates for any performance degradation from increased data rate. However, there are two remaining characteristics – one has an adverse effect and the other provides an advantage.

One characteristic is due to the fact that the SBAS satellite navigation signal passes through a signal transponder rather than being derived from an on-board satellite clock, as is the case in a GNSS satellite. Hence, the phase of the SBAS signal offset is controlled from the SBAS service provider Ground Uplink Station (GUS). Therefore, the signal inherently does not have absolute code/carrier coherency, and the sigma-phase data will never be as good as that received from a GNSS signal, especially the longer-term statistics (10 – 60 seconds). One-second and three-second statistics are maybe adequate, but still not as good as from the GNSS satellites. However, strong phase scintillation magnitude will exceed the phase noise from transponders oscillator.

Another characteristic – multipath effects on the S4 amplitude statistics – is more error-free than that of the GNSS satellites. This is not because there is less multipath present on SBAS signals. It is because the multipath is more that of a "standing wave" multipath whose fading effects vary very slowly and are essentially removed in the detrending of the amplitude data. This is not the case for GNSS amplitude data -- multipath fading is the primary source of error as the frequency content is similar to that of amplitude scintillation, albeit at a lower level. Reduction of this fading in the GPStation-6 is described later.

D. Advanced Receiver Technology

The phase noise of the reference oscillator is of crucial importance as it can easily dominate the overall phase measurement limiting the ability to measure the phase scintillation variations. As with GSV4004X series, the GPStation-6 receiver has a built-in ultra stable low phase-noise 10 MHz OCXO as frequency reference. The use of OCXO ensures that the oscillator phase noise does not obscure the effects of low level phase scintillation.

The GSV4004X series and the GPStation-6 receiver provide the same raw and detrended amplitude and phase data, and are truly backwardly compatible. However, new data logs have been defined and implemented in the GPStation-6, making data collection much more efficient by requiring less data storage. But, for users of the GSV4004X equipment, the transition to the GPStation-6 is less painful from a data collection point of view because the legacy logs are still available.

Multipath, if not mitigated, has a large impact on the amplitude scintillation measurement as it causes fading of the received signal due to constructive and destructive combination of the direct and delayed signals. The GPStation-6 receiver uses the proprietary pulse aperture correlator (PAC^{TM}) multipath mitigation technology that effectively limits magnitude of multipath error to within 5 metres [28]. More importantly, it reduces the fading that can be interpreted as amplitude scintillation. Therefore, the power measurements used for the amplitude scintillation indices are taken closer to the signal code-correlation peak.

IV. IONOSPHERIC SCINTILLATION MEASUREMENTS

Ionospheric measurements were obtained during quiet and scintillating ionospheric conditions at both equatorial and northern regions. The ionospheric indices as well as the TEC values were recorded for both GSV4004B and the GPStation-6 GISTM receivers. Figure 1 shows the geographical locations, where the ionospheric measurements were made. The latitude for Calama (Chile) is around 22^0 South, which puts it in the band of equatorial anomaly. The latitude of Calgary (Canada) is approximately 51^0 North, which is near the auroral latitudes. The measurement setup in Calama used independent but similar antennas for the GISTM receivers that were separated over a short baseline (~ 20 m). On the other hand, the measurement setup in Calgary used the same antenna for both the GISTM receivers.
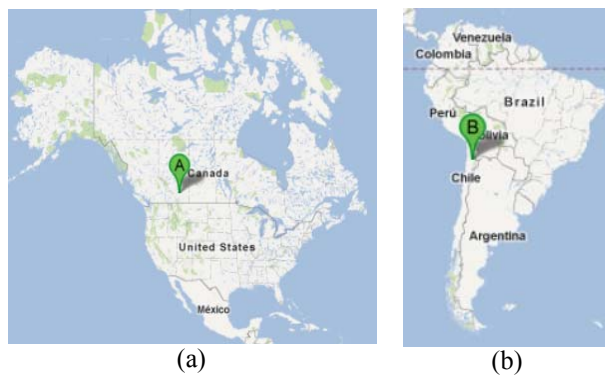

Figure 1 Map showing the locations of the measurement campaign. (a) Calgary, Canada (b) Calama, Chile

A. Tracking Performance

The average C/N$_0$ measured for GPS satellites over Calgary, Canada is shown in Figure 2. The GPS L2C and L5 signals used the pilot component for coherent carrier tracking. The

GPS L2 P(Y) was tracked using a proprietary semi-codeless tracking technique. As expected, the GPS L5 signal exhibited higher C/N$_0$ from higher transmitted power. The GPStation-6 reported C/N$_0$ was less than GSV4004B reported C/N$_0$ levels. This is mainly attributed to the wider front-end and the different noise floor estimation method implemented in GPStation-6 receiver. It should be emphasized that the wider front-end enabled tracking of multiple GNSS constellations.
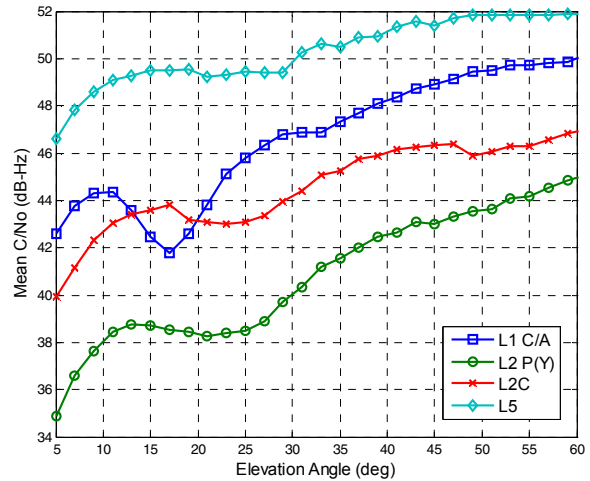

Figure 2 Measured C/No for GPS SV 25 over Calgary, Canada

The GPStation-6 provides maximal benefit by tracking multiple GNSS constellations. To illustrate this, the number of satellites that were tracked over 24 hour's period is plotted in Figure 3. With 120 channels, the GPStation-6 tracked most GPS and GLONASS satellites, which readily doubles the number of ionospheric pierce points. It also tracked the Galileo GIOVE A/B satellites at E1 and E5 when visible. On the other hand, the GSV4004B receiver is designed with 10 GPS channels and 3 SBAS channels.
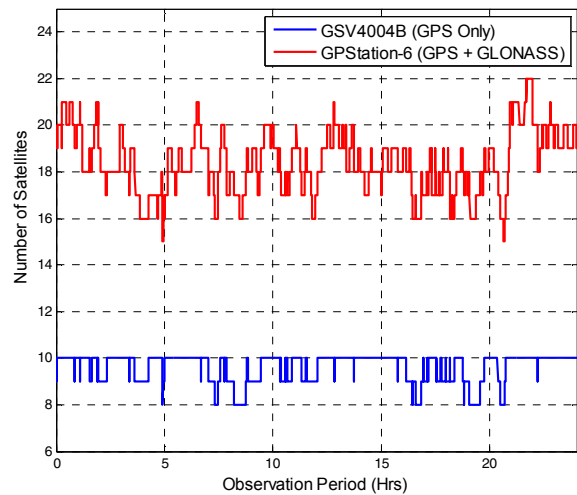

Figure 3 Number of satellites tracked over 24 hour period over Calgary, Canada for GPstation-6 and GSV4004B GISTM receiver.

B. TEC Measurements

The TEC measurement process in the GPStation-6 is identical to that in the GSV4004X receivers, providing both raw (1 Hz) and smoothed TEC data. The advantage of the GPStation-6 is that TEC can also be measured using the L2C and/or L5 signals on modernized GPS satellites, and on similar signals on GLONASS, Galileo and Compass satellites. Figure 4 and Figure **5** show plots of TEC (raw and smoothed) for both the L2P(Y) and L2C signals for PRN 29 on a recent satellite pass.
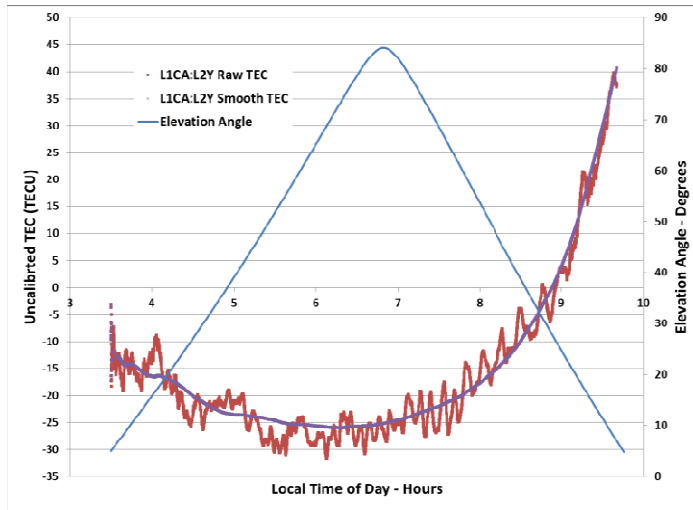

Figure 4 Measured (Uncalibrated) TEC Using PRN 29 L1C/A and L2P(Y) Signals
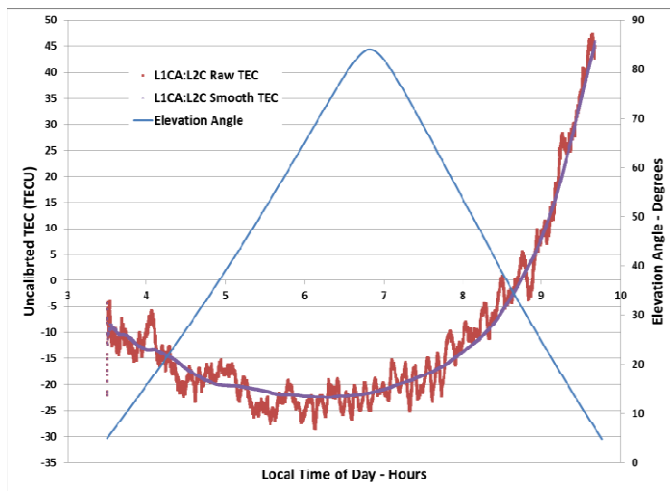
Figure 5 Measured (Uncalibrated) TEC Using PRN 29 L1C/A and L2C Signals

Note that the noise levels are similar between TEC measurements from L1 C/A – L2C and L1 C/A – L2P(Y). This is because, on the current Block IIRM satellites, the L2C power is 1.5 dB stronger than the P(Y) signal, but then is effectively reduced by 3 dB because of I/Q multiplexing. Much of the raw TEC error is due to multipath, which can be seen from the lower frequency characteristics. Although the P(Y) has a higher chipping rate, multipath mitigation technology is implemented on L2C, and L2C code tracking

loop bandwidth is a bit higher. The combination of signal power differences and multipath effects result in nearly equal noise performance.

The TEC plots in Figure 4 and Figure **5** are "Uncalibrated TEC" measurements, and thus exhibit a large TEC bias. This is due to group delay through the receiver's frontend, and some from a possible bias in the GPS SV 29 transmission. These biases can be determined by comparing night-time (local midnight to about 6 AM) TEC measured from high-elevation satellites and comparing the measurements to a "trusted" TEC model. For example, the famous Klobuchar model estimates night-time vertical TEC to be about 10 TECU. Part of that difference could be due to a bias in the satellite, but certainly, most of it is due to filtering within the GPStation-6. The wideband P(Y) signal is delayed more than the narrower band L2C signal. This differential delay (about 3.5 TECU) may be consistent from unit to unit. Time and experience will tell. Total delay, not counting satellite delay, is about 32.5 TECU for the L2C signal and 36.0 TECU for the P(Y) signal.

Comparing Figure 4 and Figure **5**, we see that the satellite pass starts at about 3:30 AM local time, and continues to nearly 10 AM. The reduction in TEC during the early morning hours is due to the rising elevation angle, leveling off at about 6 AM when the warming of the ionosphere starts taking over, cancelling the effect of the elevation angle. After that, the rise in TEC is essentially due to the heating of the ionosphere.

C. Ionospheric Scintillation Measurements

The measured amplitude scintillation index from GPS signals during the period of high ionospheric activity is plotted in Figure 6. The measured phase scintillation index is shown in Figure 7. The ionospheric scintillation predominantly occurred during the post sunset period, which extended up to 4 hours. Both the GSV4004B and GPStation-6 receivers reported amplitude and phase scintillation indices that were similar. The amplitude and phase scintillation is mainly attributed to the post sunset Equatorial ionospheric discharge.
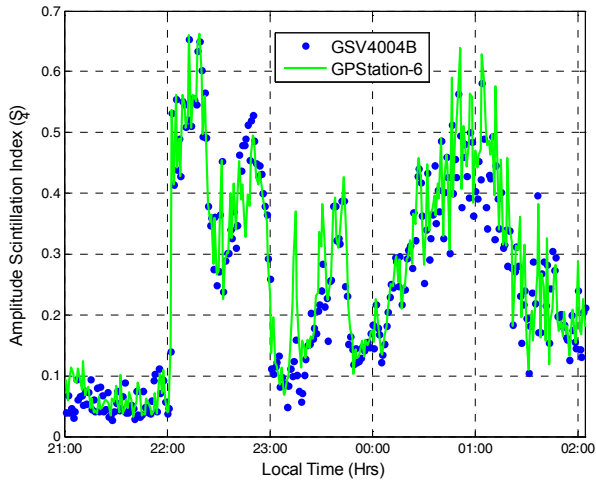
Figure 6 Measured amplitude scintillation index during active ionospheric activity at Calama, Chile (GPS PRN 25, L1 C/A)
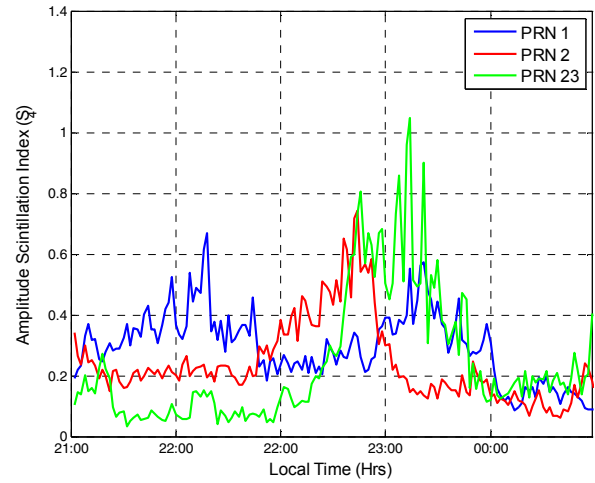
The measured amplitude and phase scintillation indices from multiple GLONASS L1 signals are shown in Figure 8 and Figure **9**. GLONASS PRN 1 ionospheric measurements readily correlated with the GPS PRN 25 between 22:00 and 23:00 hours. Similar correlation can be found between GPS PRN 25 and GLONASS PRN 23 between 23:00 and 00:00 hours. More importantly, tracking both GPS and GLONASS signals readily maximizes the ionospheric monitoring period.

Figure 7 Measured phase scintillation index during active ionospheric activity at Calama, Chile (GPS PRN 25, L1 C/A)

Figure 8 Measured amplitude scintillation index from GLONASS L1 signals during active ionospheric activity at Calama, Chile

As discussed earlier, the GPStation-6 is capable of measuring the amplitude and phase scintillation indices on the SBAS signal received from geostationary satellites in Equatorial region. Figure 10 shows the measured amplitude scintillation index from WAAS PRN 133 and 135 satellites. The time offset between the PRNs readily shows the scintillation passing below the GEOs. Besides, the amplitude scintillation measurements from SBAS satellites were consistent with both GPS and GLONASS measurements. The SBAS observations from GEOs, is particularly useful for characterizing the equatorial ionosphere scintillation phenomenon continuously. On the other hand, the use of phase scintillation measurements from SBAS signals is limited due to GEO transponder oscillator phase noise. Figure 11 shows the measured phase scintillation from WAAS PRN 133 and 138 satellites. The phase measurement although noisy signifies the ionospheric effects particularly between 21:00 and 22:00 hours.
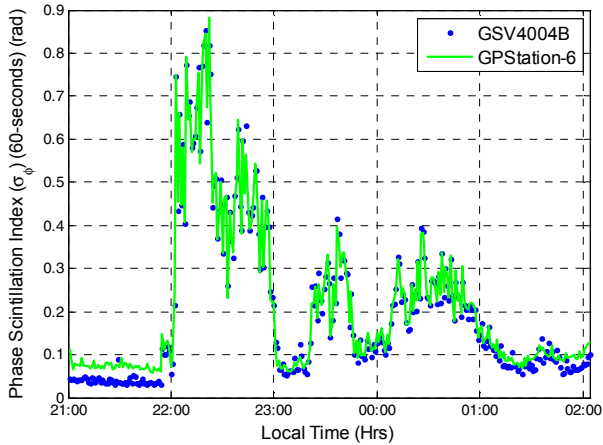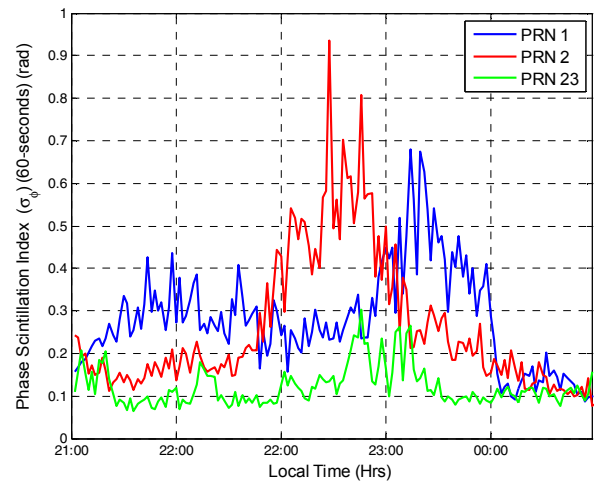

Figure 9 Measured phase scintillation index from GLONASS L1 signals during active ionospheric activity at Calama, Chile
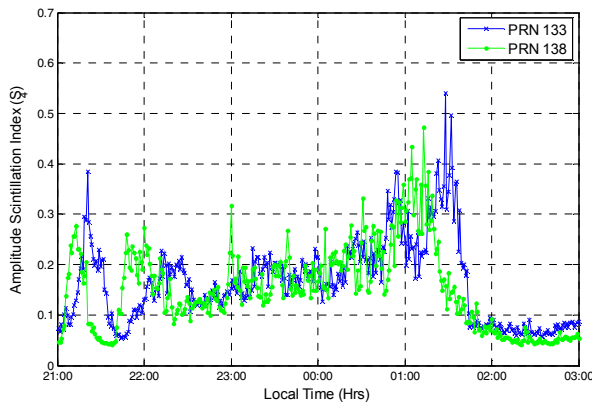
Figure 10 Measured amplitude scintillation index during active ionospheric activity at Calama, Chile (WAAS L1 C/A)
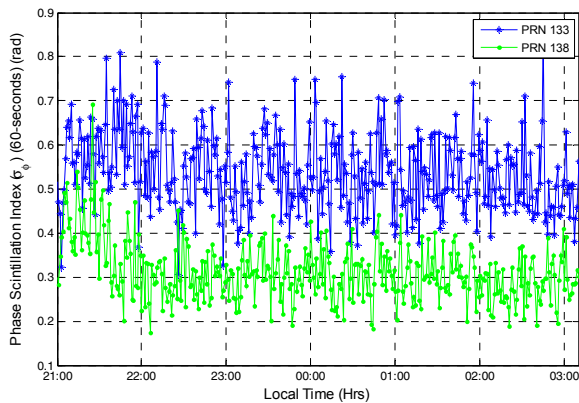

Figure 11 Measured phase scintillation index during active ionospheric activity at Calama, Chile (WAAS L1 C/A)

V. CONCLUSION

GNSS signals although vulnerable to ionospheric scintillation provides an excellent mean to measure the same ionospheric effects on radio signals continuously. Incorporating NovAtel's multi-constellation, multi-frequency GNSS measurement engine and an ultra low-noise OCXO, the GPStation-6 enables comprehensive ionospheric scintillation and TEC monitoring. It is also backward compatible with the mature GSV4004B receivers used for ionospheric monitoring worldwide. Preliminary measurements results during recent ionospheric activity corroborated the validity and efficacy of GPStation-6 GISTM receiver.

REFERENCES

[1]   Gleason S., Gebre-Egziabher D.: GNSS Applications and Methods. Artech House. Boston/London,2009.

[2]   Aarons, J., Klobuchar, J. A., Whitney, H. E., Austen, J., Johnson, A. L., and Rino, C. L., "Gigahertz scintillations associated with equatorial patches," Radio Science, Vol. 18, No. 3, 1983, pp. 421–434.

[3]   RTCA, Inc., Minimum Operational Performance Standards for Global Positioning System/Wide Area Augmentation System Airborne Equipment, RTCA DO-229D, December 13, 2006.

[4]   Kaplan, E. D., and Hegarty, C. J., Understanding GPS Principles and Applications, 2 ed. Norwood: Artech House Inc., 2006.

[5]   Klobuchar, J. A., "Ionospheric Effects on GPS," Global Positioning System: Theory and Applications, edited by B. W. Parkinson and J. J.

Spilker, American Institute of Aeronautics and Astronautics, Washington, DC, 1996, pp. 485–515.

[6]   Groves, K.M., S. Basu, E.J. Weber, M. Smitham, H. Kuenzler, et al, Equatorial scintillation and systems support, Radio Sci., 32, 2047–2064, 1997.

[7]   R. Langley, R. B. "GPS, the ionosphere, and the solar maximum, GPS World", 11(7), 44–49, July 2000.

[8]   Kintner Jr., P.M., Humphreys, T., and Hinks, J., "GNSS and Ionospheric Scintillation – How to Survive the Next Solar Maximum", Inside GNSS, July/Aug 2009, pp. 22-29.

[9]   Skone, S., "Wide Area Ionosphere Grid Modeling in the Auroral Region", UCGE Reports Number 20123, Ph.D thesis, The University of Calgary, Calgary, Alberta, Canada. 1998.

[10] Kelley, M.C., The Earth's Ionosphere: Plasma Physics and Electrodynamics, Academic Press, San Diego, CA, 1989.

[11] Doherty, P. H., Delay, S. H., Valladares C. E., and Klobuchar, J. A., "Ionospheric Scintillation Effects in the Equatorial and Auroral Regions." in Proceeding of ION GPS-2000, Salt Lake City, UT, September 2000.

[12] Conker, R.S., El Arini, M.B., Hegarty, C.J., and Hsiao, T., "Modeling the effects of ionospheric scintillation on GPS/SBAS availability", Radio Sci., 38 (1), DOI: 10.1029/2000RS002604, 2003.

[13] Humphreys, T.E., Psiaki, M.L., Ledvina, B.M., and Kintner, P.M., GPS carrier tracking loop performance in the presence of ISs, Proc. ION GNSS 2005, Institute of Navigation, Long Beach, CA, 2005.

[14] Jakowski, N., Mayer, C., Hoque, M.M., and Wilken V., "Total electron content models and their use in ionospheric monitoring"Radio Science, vol. 46, No. 18, RS0D18, doi:10.1029/2010RS004620, 2011.

[15] WAAS MOPS, Minimum Operational Performance Standards for Global Positioning System/Wide Area Augmentation System Airborne Equipment, RTCA Inc. Document No. RTCA/DO-229B, October 6, 1999, p. 225.

[16] Komjathy, A., Mannucci, A.J., Sparks, L., Coster, A. The ionospheric impact of the October 2003 storm event on WAAS. GPS Solutions 9, 41−50, 2005.

[17] Warnant, R., Lejeune, S., Bavier, M., 2007. Space weather influence on satellite-based navigation and precise positioning. In: Lilensten, J. (Ed.), Space Weather—Research towards Applications in Europe, Astrophysics and Space Science Library series, vol. 344, Springer, pp. 129–146.

[18] Woo, K.T.. Optimum semi-codeless carrier phase tracking of L2, Proceedings of the ION GPS-99, Nashville, Tennessee, September, 1999.

[19] Van Dierendonck, A. J., Klobuchar, J., and Hua, Q., "Ionospheric Scintillation Monitoring Using Commercial Single Frequency C/A Code Receivers," Proceedings of ION GPS-93, Salt Lake City, UT, September 1993, pp. 1333 - 1342.

[20] Morrissey, T. N., Shallberg, K. W., Van Dierendonck, A. J., and Nicholson, M. J., "GPS receiver performance characterization under realistic ionospheric phase scintillation environments," Radio Sci., Vol. 39, 2004, pp. 1–18.

[21] Van Dierendonck, A. J., Hua, Q., Fenton, P., and Klobuchar, J., "Commercial Ionospheric Scintillation Monitoring Receiver Development and Test Results," Proceedings of the 52nd Annual Meeting, The Institute of Navigation, Cambridge, MA, June 1996, pp. 573 - 582.

[22] GPStation-6, GNSS Ionospheric Scintillation and TEC Monitoring (GISTM) Receiver – User Manual, OM-20000132, 2011.

[23] Van Dierendonck, A.J., and Arbesser-Rastburg, B., "Measuring Ionospheric Scintillation in the Equatorial Region Over Africa, Including Measurements From SBAS Geostationary Satellite Signals," Proc. ION GNSS 2004, Long Beach, CA, Sept. 21-24, 2004, pp. 316-324.

[24] Van Dierendonck, A.J., and Arbesser-Rastburg, B., "Measuring Ionospheric Scintillation in the Equatorial Region Over Africa, Including Measurements From SBAS Geostationary Satellite Signals," Proc. ION GNSS 2004, Long Beach, CA, Sept. 21-24, 2004, pp. 316-324.

[25] Tran, M., and Hegarty, C., "Performance Evaluation of the New GPS L5 and L2 Civil (L2C) Signals", Navigation: Journal of the Institute of Navigation, Vol.51, No.3, Fall 2004.

[26] IS-GPS-200F, GLOBAL POSITIONING SYSTEM DIRECTORATE SYSTEM ENGINEERING & INTEGRATION INTERFACE SPECIFICATION, 20 September 2011.

[27] IS-GPS-705A, GLOBAL POSITIONING SYSTEM WING (GPSW) SYSTEMS ENGINEERING & INTEGRATION INTERFACE SPECIFICATION, 8 June 2010.

[28] Jones, J., Fenton, P., and Smith, B., "Theory and Performance of the Pulse Aperture Correlator," NovAtel Inc., 2004. (http://webone.novatel.ca/assets/Documents/Papers/PAC.pdf)